

# **PERFORMANCE OF STAINLESS STEEL AISI 304 WIRE REINFORCED METAL MATRIX COMPOSITES MADE USING ULTRASONIC ADDITIVE MANUFACTURING IN BENDING**

David O. Jarrett, James M. Gibert<sup>1</sup>, Georges M. Fadel

Department of Mechanical Engineering, Clemson University

## **ABSTRACT**

Ultrasonic additive manufacturing (UAM) is a solid-state additive and subtractive manufacturing process that utilizes ultrasonic energy to produce layered metallic parts. The process is easily extended to create advanced multi-material structures, e.g., metal matrix composites, functionally graded metallic components, and shape memory alloys. This research utilizes a three point bending test to compare the elastic modulus in metal matrix composites (MMC's) specimens consisting of stainless steel wire reinforcements with an aluminum matrix to unreinforced test specimens; both specimens are produced by UAM. In the MMC the volume fraction of wire is relatively low, 0.77%, yet yields an average increase in modulus of 8.9%.

## **INTRODUCTION**

Ultrasonic Additive Manufacturing also known as Ultrasonic Consolidation (UC) is a solid state manufacturing process that produces layered metallic components from a combination of ultrasonic welding and contour milling. Figure 1 is a visual representation of the primary components used in UAM. The machine consists of an ultrasonic horn

---

<sup>1</sup> Corresponding author

also called a sonotrode, piezoelectric transducer, and booster to amplify vibrations, a heater, and a movable base. The process begins with the placement of a thin metal foil, typically 5.90 mil (150  $\mu\text{m}$ ) thick and 0.94 inches (23.88 mm) wide, on a sacrificial base plate. Prior to the deposition of the foil, the base plate is in turn bolted downward and heated to 300°F or approximately 150°C. During the welding process the sonotrode compresses and rolls over the foil while simultaneously vibrating transversally at a nominal frequency of 20 kHz and at amplitudes ranging from  $1.97 \times 10^{-1}$  to 1.18 mils (5-30  $\mu\text{m}$ ). After the foil is bonded, the process is repeated for additional foils adding new layers until the final size of the component is reached. The consolidated foils are machined as needed to produce the desired final part geometry. The commonly accepted theory for the mechanism of bonding is that during welding, the surface contaminants of both materials are removed, allowing direct metal-to-metal contact and producing sufficient stress to create plastic flow resulting in a metallurgical bond [1]. The primary foil material used for this process is Al 3003 H-18, however UAM is not limited to this material. Other metals such as copper, titanium, stainless steel and brass have also been welded together.

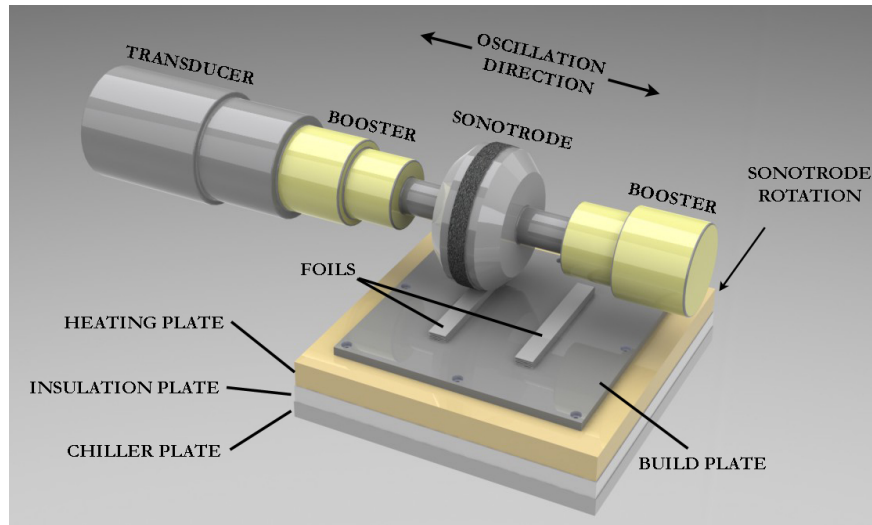


**Figure 1: Basic schematic of the UAM process (not to scale).**

In recent years, few studies have attempted to determine the mechanical properties of parts built using the UAM process. Most studies have focused on optimizing process parameters to maximize the bonding area and peel strength of the initial bonds [2-4], studying the apparent build limit of the process, [5-9], developing and performance MMCs using UAM [10-13], and methods the placement of wires in the matrix of the MMC [14]. Leagon [15] examined the interlaminar shear strength of standard parts built with various orientations.

Particularly relevant to this work are the studies performed by Ram *et. al* [16] and Yang *et. al* [17]. The work by Ram *et. al* [16] is a comprehensive study demonstrating that materials such as Al alloy 2024, Inconel 600, Brass, and Stainless Steel AISI 347 can be successfully bonded to Al alloy 3003 foils. This work also proved that it is possible to embed SiC and MetPreg fibers, and Stainless Steel AISI 304 wire mesh in Al alloy 3003 foils.

Yang *et. al* [17] extended the work Ram *et. al* [16] by embedding SiC fibers within UAM parts. The researchers then evaluated the resulting MMC's mechanical properties compared to parts produced without fiber. In their tests the reinforced parts consisted of fibers running in the lateral direction of the foil. Peel tests, tensile tests, and three point bending tests were used to evaluate each type of part, to determine maximum peeling load, tensile test and interlaminar shear strength. The reinforced parts yielded better higher peeling loads, tensile tests but lower interlaminar shear strength when compared to the unreinforced UC parts.

The present study quantifies the effective flexural modulus of a MMC produced from stainless steel wire and Al 3003 matrix through a three-point bending test. The effective flexural modulus of the MMC is compared to the flexural modulus of an unreinforced test specimen also produced by UAM. It is worth noting that in composites the tensile and flexural modulus may not be equal. The flexural modulus is dependent on ply stacking sequence of the laminate. The manuscripts begin with an experimental plan detailing the materials used in this study, the development of a specialized wire placement fixture, and a description of the three point bending test used to determine the modulus of the specimens. Next, it presents the results of the bending test, compares the predictions to theoretical predictions from the rule of mixtures. The manuscript ends with a discussion of future work and concluding thoughts.

## **EXPERIMENTAL TESTING PLAN**

This study utilized thermally stabilized 3003-H18 aluminum foils supplied by the United Aluminum Corp., North Haven, Connecticut. The foils were 150  $\mu\text{m}$  thick and 0.94 inch or 23.88 mm wide. We used stainless steel AISI 304 wire (75  $\mu\text{m}$  diameter) supplied by Goodfellow Materials. The modulus varies from 190 to 210 GPa.

### **WIRE PLACEMENT FIXTURE**

The test presented in this manuscript required a custom wire placement fixture to hold the wire at the proper angle orientation and position. Ideally, the fixture should be constructed of low cost materials, allow for wires to be placed at various angles, orientations and wire spacing. Additionally, it must be durable enough to withstand frequent handling.

Using the above criteria, the frame of the fixture is made of 9 separate, 0.25 in. x 0.25 in. x 12 in. brass tubes. The fixture consists of 7 tubes running along its length attached to 2 tubes that form its sides. The inner tubes are attached to the outer tubes by threaded rods. This effectively forms 6 slots allowing the jig to accommodate the manufacture of 6, 0.94 in wide specimens. A small channel is cut down the middle of one side of each tube over the entire length, the wire could be held in with claw like features, preventing the wire from sliding out and coming loose, Figure 2.

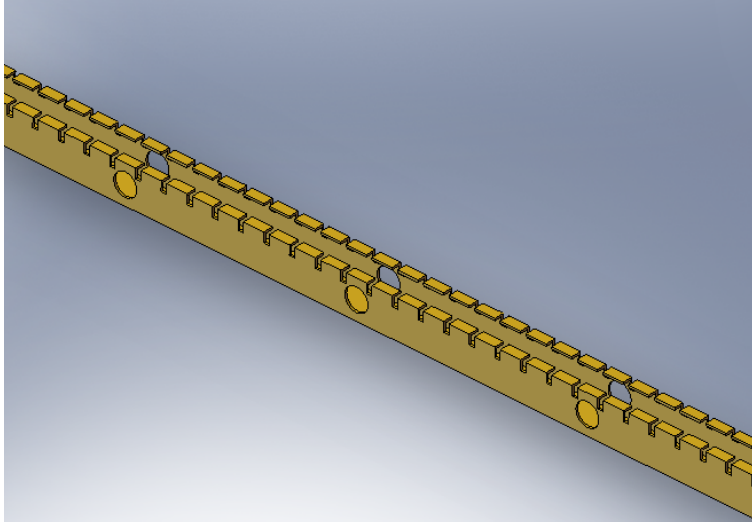


**Figure 2: Detailed view of fixture.**

The “claws” were made by using a wire EDM to cut 0.167 in. slots perpendicular to the length of each tube. Figure 3 shows a picture of the wire placement jig with wire in place.



**Figure 3: Wire fixture with wire properly placed, ready to be embedded.**

## FABRICATION OF BENDING TEST SAMPLES

The shape and size of the bending test specimens was determined in accordance with ASTM D 790-10 [18] standard with and without embedded SS 304 wire. Each specimen is of length 3.0 in., width 0.625 in., and thickness 0.125 in. The specimen is tested over a support span of 2.5 inches. Ideally, we would like a span to thickness ratio of 60 to 1 to negate the effects of shear. However, in this study we are comparing the effects of the reinforcement to normally produced UAM specimens and not focused on quantify the exact flexural modulus. The following process parameters were used in the ultrasonic welding of the specimens: amplitude of 14 microns, welding speed of 32.0 mm/s and a normal load of 1450 N. For this first test, we restrict the orientation of the wires to run along the length of the specimen. Figure 4 shows the arrangement of the wire in the MMC; 2 wires form a group and 4 groups span the cross section of the MMC.

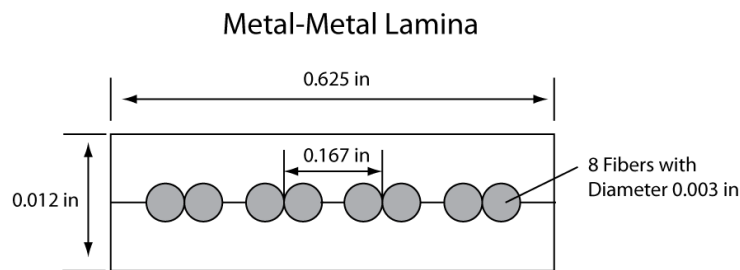


**Figure 4: Arrangement of stainless steel wires in MMC.**

Each group is spaced out 0.167 in. from center to center allowing for a total of 8 wires to be embedded. Furthermore we embedded wires every other layer, resulting in a total of

88 wires over the thickness of the sample; a volume fraction of wire in the specimen is 0.77%. A photograph of the reinforced samples can be seen in Figure 5.

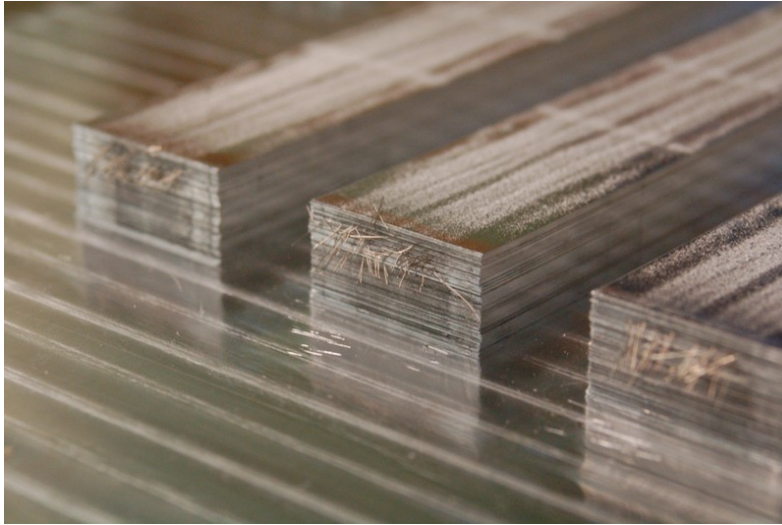


**Figure 5: Wire reinforced samples before machining.**

Once the specimens were produced by UAM, they were then cut out into their overall shape using a MAXIM 1500 waterjet. Finally, the specimens were machined to the final thickness of 0.125 in., as shown in Figure 6.



**Figure 6: Test samples after being cut on the water jet.**

When machining to the final dimensions, first the base plate and excess consolidated specimen was removed using a band saw with a wax-lubricated blade. The lubrication prevented the Al 3003 from becoming embedded into the saws teeth. Once the rough cut was made with the band saw, the final thickness was achieved using a fly cutter. Using this tool, 0.015 in. of material was removed at each pass until the desired thickness of 0.125 in. was reached. Due to the difficulty of machining Al 3003 precautions were taken to keep the material from overheating by constantly “flooding” the cutting tool with cooling fluid. Finally, the specimens were polished on all surfaces to remove any surface imperfections and scratches, Figure 7.



**Figure 7: Final appearance of a test specimen.**

### **MECHANICAL TESTING**

The mechanical testing of the specimens is based on a three point bending test from the ASTM D790 standard [18]. The standard is for fiber-reinforced plastics, however, the equations covering strain and stress are valid since they are derived principles from strength of materials assuming elastic, and elastic-plastic material behavior.

In determining the elastic modulus, several quantities are needed: the rate of crosshead travel of the press used in the test, the maximum stress at the midpoint of the specimen along its outer surface, and the corresponding strain at the same point. The tests were conducted on a hydraulic press at a strain rate of 0.01 in./min. The rate of crosshead [18] travel,  $R$ , necessary to achieve this strain rate given the geometry of the test sample is given by [18]

$$R = \frac{ZL^2}{6d}, \quad (1)$$

where  $Z$  is 0.01 for the desired strain rate,  $L$  is span length, 2.5 in., and  $d$  is the thickness of the part, 0.125 inches. The resulting cross head travel speed is calculated to be 0.083 in./min. The stress [18] during the bend test is defined as:

$$\sigma = \frac{3PL}{2bd^2}, \quad (2)$$

where  $P$  is the load in lbf, and  $b$  is the width, 0.625 inches. The corresponding strain [18] is calculated from:

$$\epsilon = \frac{6Dd}{L^2}. \quad (3)$$

Finally, the elastic flexural modulus [18] is defined as

$$E_B = \frac{L^3m}{4bd^3}, \quad (4)$$

where  $m$  equals load  $P$  divided by deflection at the midpoint  $D$  and is the slope of the straight-line portion of the load deflection curve. The moduli are calculated for both specimens (with and without imbedded wires) and compared to see if the wire reinforcements actually increase or reduce the flexural modulus  $E_B$ . Figure 8 shows the sample in the bending fixture.

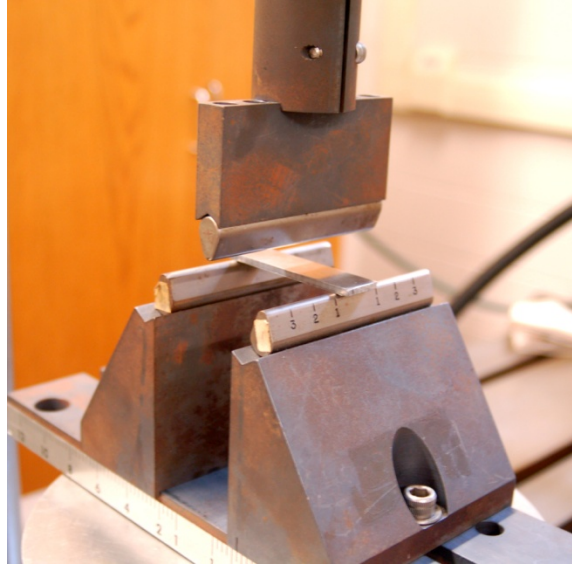


**Figure 8: Three point bend test loading apparatus with specimen.**

### RESULTS AND DISCUSSIONS

During testing, the samples were loaded within the region elastic behavior and not to yielding or fracture. The stress and strain experienced by the specimen during the experiment are calculated using Eqn. (2) and (3). A linear least squares regression line was fit through the data points for the load-deflection curve of of each sample, the slope of this line is

$$m = \frac{\sum_{i=1}^n (x_i - \bar{x})(y_i - \bar{y})}{\sum_{i=1}^n (x_i - \bar{x})^2}, \quad (5)$$

applying this equation to bending test,  $n$  is the number of data points and the data pairs  $(x_i, y_i)$  represent the experimental deflection and load,  $\bar{x}$  and  $\bar{y}$  are their respective

means. Figure 9 shows a typical stress-strain curve using Eqns. (2) and (3) along with resulting stress-strain curves from fitting the load-deflection curve from a reinforced and unreinforced sample. The gray and blue dots represent the stress strain curve dot for an unreinforced sample, and reinforced sample, respectively. Similarly, the gray and blue lines represent a linear fit of stress strain data for unreinforced sample, and reinforced sample, respectively. It is clear that the load tested, both samples exhibit a linear response. The slope of the two lines differs indicating that the samples have different elastic moduli. The highlighted relationships on the plot give the one-dimensional constitutive relationship for each sample, blue indicates the reinforced sample and gray the unreinforced sample.

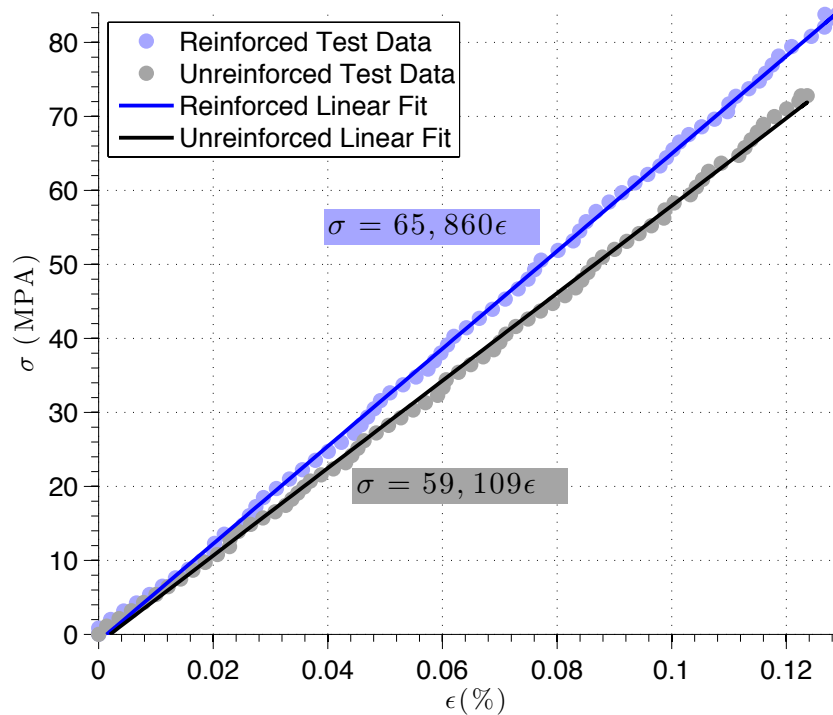


**Figure 9: Raw stress strain data and curve fits used to determine flexural modulus**

The samples were loaded 4 different times in order to evaluate the repeatability of the testing conditions. The results from these 4 tests were averaged together to get a representative value of each specimen. A total of 4 different specimens were tested, 2 of each type of part, reinforced and unreinforced. Figure 10 presents the results from these tests. The bars give the values of modulus for each test and sample; the dashed blacked line indicates the average of the reinforced and unreinforced samples. The first thing to note is the modulus varies from sample to sample. The most notable being variation is between unreinforced samples 1 and 2. It is not readily apparent why this change occurs. It could be due to numerous conditions such as the cleanliness of the horn during the manufacturing process, or variation in the modulus and surface condition of the foil. Changes in the previously mentioned parameters would affect bonding and thus the effective flexural modulus of the specimen. However, in all the tests the reinforced samples have a larger flexural modulus.

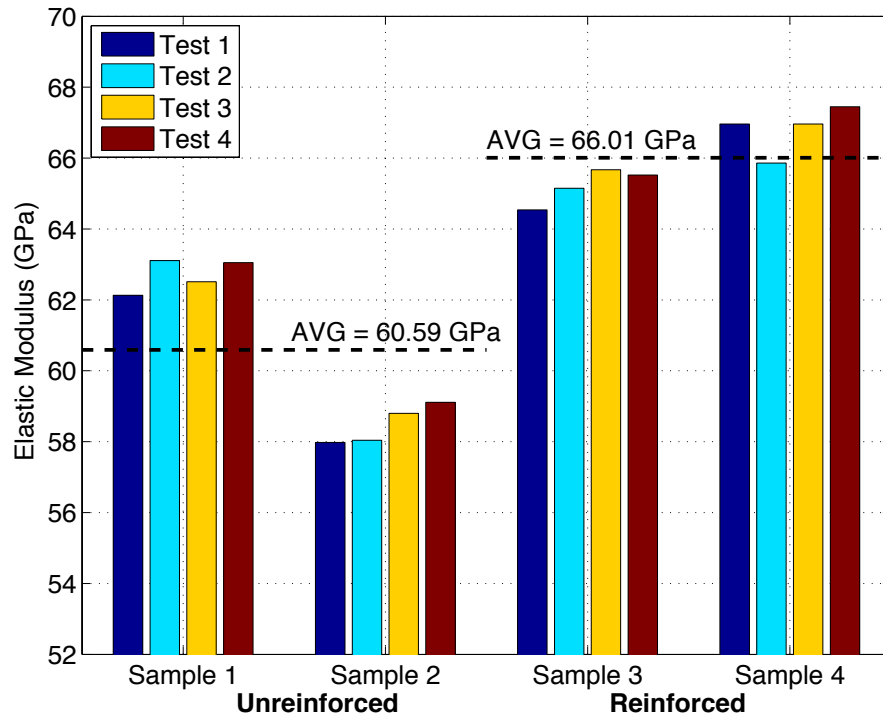


**Figure 10: Elastic modulus results of the unreinforced and reinforced samples.**

The average modulus of the unreinforced samples is 60.59 GPa, while material references list Al 3003 as having a 68.9 GPa modulus [19]. This significant difference most likely lies in the fact that the parts tested are made using the UAM process, even the unreinforced ones. Assuming some percentage bonding in the layers, a material with lower bulk modulus would be expected due to voids. If a solid, homogenous sample of Al 3003 was tested, the results achieved in this testing might have been closer to the reference value. The reinforced samples have an average modulus of 66.01 GPa. Overall, there is an 8.9% increase in modulus between the reinforced samples and the nominal samples. Again, it should be noted that this improvement might be exaggerated due to variation in modulus between the unreinforced samples. More samples are needed to

obtain a complete analysis of the actual increase in modulus. However, this increase in modulus of the MMC at low fiber volume is either due to the modulus of the wire being nominally 2.79 times that of the foil or the development of strain hardening region around the fiber weld interface effectively changing the matrix in the bonding region [20].

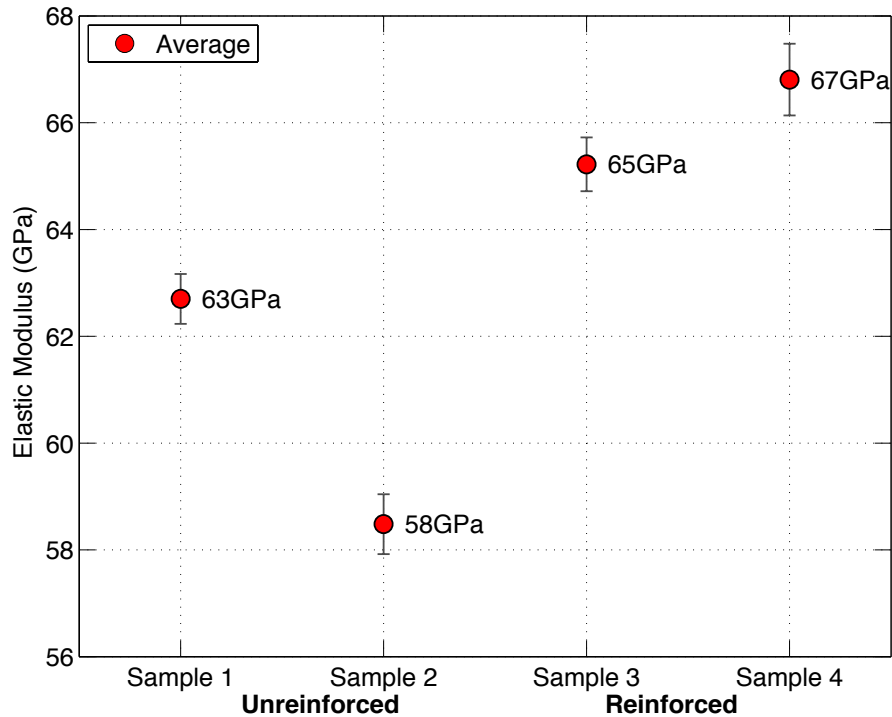


**Figure 11: Error bar plot for modulus to determine repeatability in loading – bare represents one standard deviation from average.**

Figure 11 examines the variation in modulus in each sample due by plotting the mean and the standard deviation of the modulus from the 4 tests. While the average modulus of the samples vary in both the reinforced and unreinforced cases. If we examine all the samples the standard deviation is less than 0.7 GPa over the 4 tests indicating that the modulus of each sample is relatively constant due to bending.

Based on the present results UAM seemingly produces stainless steel wire reinforced composites that exhibit superior resistance to bending than nominally produced UAM specimens. However, further studies with increased sample size are needed to fully confirm this observation.

### **FUTURE WORK**

This research may progress along several paths. The immediate follow up to this study is to increase the sample size, perform microscopy to examine the bond along the fibers to see if a strain harden region develops along the interface, and examine the fatigue life of the composites. However, this work represents only the initial steps in quantifying the performance of MMC's produce by UAM. Our broader plans are to investigate a variety of materials, diameters, and orientations of the fiber in the MMC on its flexural and in-plane moduli, and yield strength.

### **CONCLUSION**

This manuscript considers the flexural modulus of stainless steel wire reinforced aluminum composite through a three point bending test. The samples used in this study had a relatively low volume fraction of wire, 0.77%, yet yields an average increase in modulus of 8.9% when compared to unreinforced samples. However, the increase in modulus may be skewed due to variation in modulus of the unreinforced samples.

## ACKNOWLEDGMENTS

Thank you to Dr. Laine Mears, Josh Jones and Matthew Kuttolamadom for allowing us to use the wire EDM machine to manufacture the wire placement fixture used in this work. Thank you to the ME research shop, especially Michael Justice and Jamie Cole for providing technical support and always lending a helping hand when needed.

A special thanks goes to John Ayer who developed the G-code used to build the UC parts studied in this work. Other assistance with troubleshooting issues with the machine was very helpful throughout the year.

## REFERENCES

1. O'Brien, R. L., ed., 1987) *Welding Processes*, Eighth ed., Vol. **2** of *Welding Handbook*. American Welding Society, Miami, FL.
2. Kong, C. Y., Soar, R. C., Dickens P. M., 2004, "A Model for Weld Strength in Ultrasonically Consolidated Components", *Proceedings of the Institution of Mechanical Engineers, Part C: Journal of Mechanical Engineering Science*, Vol. **219**(1), pp. 83-91.
3. Kong, C. Y., Soar, R. C., Dickens P. M., 2004, "Optimum Process Parameters for Ultrasonic Consolidation of 3003 Aluminum", *Journal of Materials Processing Technology*, Vol. **146**(2), pp. 181-187.
4. Janaki Ram, G.D., Yang, Y., Stucker, B.E., 2006, "Effect of Process Parameters on Bond Formation During Ultrasonic Consolidation of Aluminum Alloy 3003", *Journal of Manufacturing Systems*, Vol. **25**(3), pp. 221-238.
5. Robinson, C.J., Zhang, C., Janaki Ram, G.D., Sigg, E.J., Stucker B., Li, L., 2006, "Maximum Height to Width Ratio of Freestanding Structures Built Using Ultrasonic Consolidation," *Seventeenth Solid Freeform Fabrication Proceedings*, pp. 502-516.

6. Zhang, C. and Li L., 2006, "A Study of Static and Dynamic Mechanical Behavior of Substrate in Ultrasonic Welding", *Seventeenth Solid Freeform Fabrication Symposium*, pp. 502-506.
7. Zhang, C. and Li L., 2010, "Effect of Substrate Dimension on Dynamics of Ultrasonic Consolidation", *Ultrasonics*, pp. 811-823.
8. Gibert, J.M., Austin, E.M. and Fadel. G., 2010, "Effect of Height to Width Ratio on the Dynamics of Ultrasonic Consolidation", *Rapid Prototyping Journal*, Vol. **16**(5): p. 284-294.
9. Gibert, J.M., McCullough, D., Fadel, G., Martin, G., Austin, E.M., 2009, "Stick-Slip Dynamics in Ultrasonic Consolidation", *Proceedings of the ASME 2009 International Design Engineering Technical Conferences & Computers and Information in Engineering Conference (IDETC 09) San Diego, CA*.
10. Kong, C.Y., Soar, R., 2005, "Method for Embedding Optical Fibers in an Aluminum Matrix by Ultrasonic Consolidation", *Applied Optics*, Vol. **44**(30) pp. 6325-6333.
11. Hopkins, C. D., Dapino, M.J., Fernandez, S.A., 2010, "Statistical Characterization of Ultrasonic Additive Manufacturing Ti/Al Composites", *Journal of Engineering Material and Technology*, Vol. **232**
12. Hanhnlén, R., Dapino, M.J., Short, M., Graff K., 2009, "Aluminum-Matrix Composite with Embedded Ni-Ti Wires Ultrasonic Consolidation", *Industrial and Commercial Applications of Smart Structures Technologies Proceeding of the SPIE, Vol. 7290*.
13. Hanhnlén, R., Dapino, M.J., 2011, "Aluminum-Matrix Composite with Embedded Ni-Ti Wires Ultrasonic Consolidation", *Industrial and Commercial Applications of Smart Structures Technologies Proceeding of the SPIE, Vol. 7979*.
14. Masurtschak, S., Harris, R.A., 2011, "Enabling Techniques for Secure Fibre Positioning in Ultrasonic Consolidation for the Production of Smart Material Structures", *Sensors and Smart Structures Technologies for Civil, Mechanical, and Aerospace Systems, Proceedings of the SPIE*, Vol. **7981**, pp. 79810M-79810M-1
15. Leagon, J.M., 2007, "Characterization of the Interlaminar Shear Strength of Ultrasonically Consolidated Components", Clemson University, Clemson, SC.

16. Ram, G.D., Robinson, C., Yang, Y., and Stucker, B.E., 2007, "Use of Ultrasonic Consolidation for Fabrication of Multi-Material Structures", *Rapid Prototyping Journal*, Vol. **13**(4), 226-235.
17. Yang, Y., Stucker, B.E., Ram, G.D., 2010, "Mechanical Properties and Microstructures of SiC Fiber-reinforced Metal Matrix Composites Made Using Ultrasonic Consolidation", *Journal of Composite Materials*, Vol. **44**, 3179-3194.
18. ASTM Standard D790, 2003, "Standard Test Methods for Flexural Properties of Unreinforced and Reinforced Plastics and Electrical Insulating Materials, ASTM International, West Conshohocken, PA, 2010, DOI: 10.1520/D790-10, [www.astm.org](http://www.astm.org).
19. Aluminum 3003 H-18, retrieved April, 2012, [www.matweb.com/search/datasheet.aspx?matguid=91c99440833341fc8fbed26149bc35e&ckck=1](http://www.matweb.com/search/datasheet.aspx?matguid=91c99440833341fc8fbed26149bc35e&ckck=1)
20. Yang, Y., 2008, "Fabrication of Long-Fiber-Reinforced Metal Matrix Composites Using Ultrasonic Consolidation", Dissertation, University of Utah.